Measurements of the Higgs boson properties from diboson final states

Jahid Hossain on behalf of the CMS collaboration

Aug 25–29, 2025

32nd Lepton-Photon Conference - Madison

Introduction

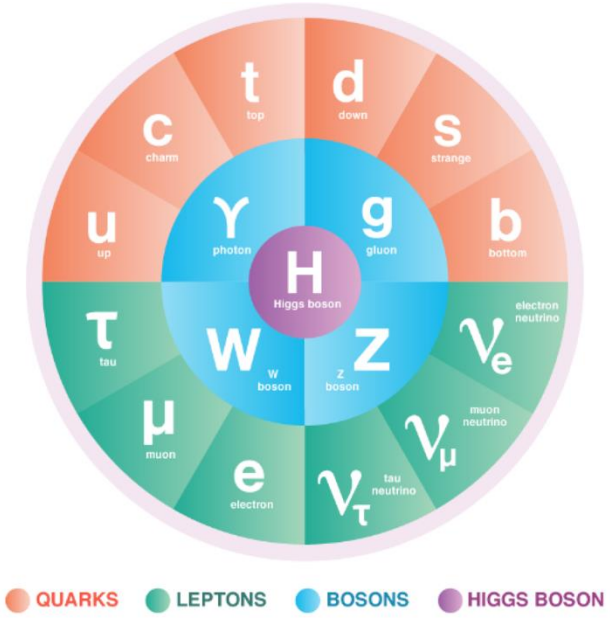

The Higgs boson, the last missing piece of the Standard Model (SM), was discovered by the CMS and ATLAS collaborations in 2012 using Run 1 LHC data

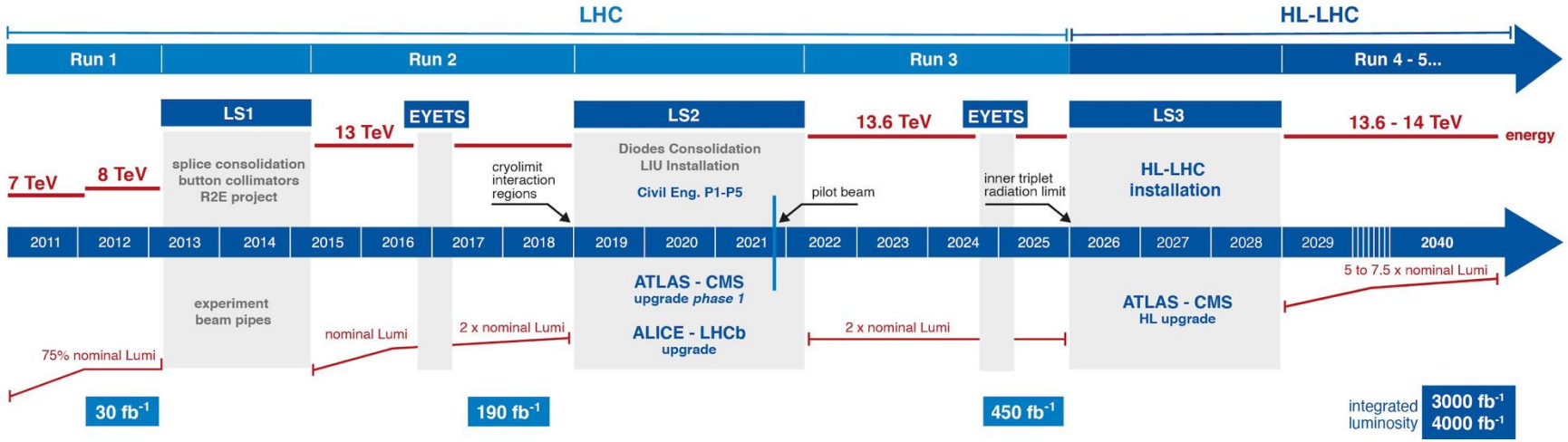

Higgs Properties:

- ✓ Mass
- ✓ Width
- ✓ Spin/CP
- ✓ Couplings
- ✓ Cross section

Run 1 :
Key Higgs properties were measured

Run 2 :
Higher precision measurements

Run 3 :
push precision further & probe for new physics

So far agree with SM predictions and any deviation would indicate new physics

Higgs Boson Production and Decay modes

With $m_H \approx 125$ GeV, a wide range of production and decay modes are accessible

Dominant production modes:
ggH, VBF

EW production modes
VBF & VH → clean signatures

Higgs decays mostly to **b-quarks**

Diboson decay modes:
$\boldsymbol{WW, ZZ, \gamma\gamma, Z\gamma}$

ZZ & $\gamma\gamma$ → clean signatures for precision measurements

Production mode	Cross section (pb)	Decay channel	Branching fraction (%)
ggH	48.31 ± 2.44	bb	57.63 ± 0.70
VBF	3.771 ± 0.807	WW	22.00 ± 0.33
WH	1.359 ± 0.028	gg	8.15 ± 0.42
ZH	0.877 ± 0.036	$\tau\tau$	6.21 ± 0.09
ttH	0.503 ± 0.035	cc	2.86 ± 0.09
bbH	0.482 ± 0.097	ZZ	2.71 ± 0.04
tH	0.092 ± 0.008	$\gamma\gamma$	0.227 ± 0.005
		$Z\gamma$	0.157 ± 0.009
		ss	0.025 ± 0.001
		$\mu\mu$	0.0216 ± 0.0004

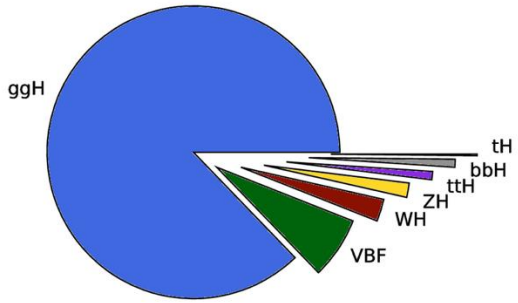

$\sqrt{s}$= 13 TeV & m_H= 125.38 GeV

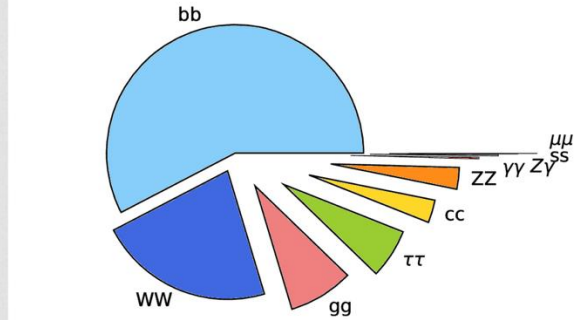

Nature 607 (2022) 60-68

Higgs Boson Production and Decay modes

With $m_H \approx 125$ GeV, a wide range of production and decay modes are accessible

Dominant production modes:
ggH, VBF

EW production modes
VBF & VH → clean signatures

Higgs decays mostly to **b-quarks**

Diboson decay modes:
$\boldsymbol{WW, ZZ, \gamma\gamma, Z\gamma}$

ZZ & $\gamma\gamma$ → clean signatures for precision measurements

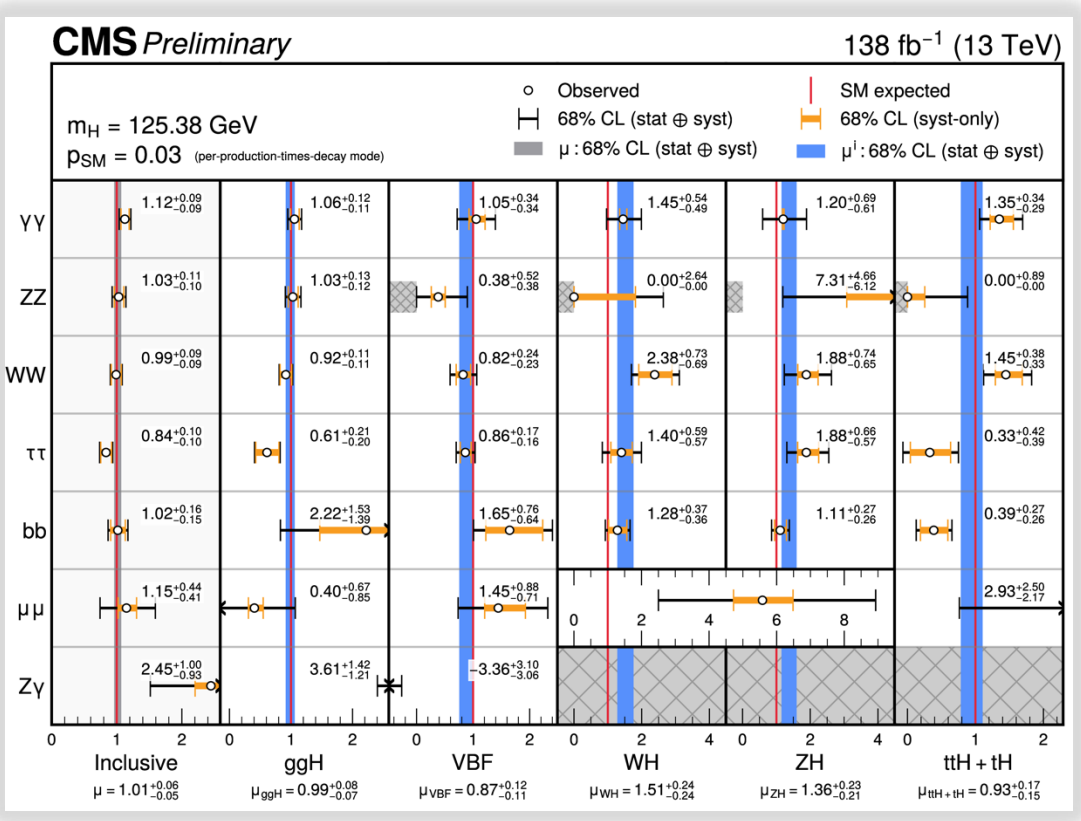

CMS-PAS-HIG-21-018

- Summary of the signal-strength modifier measurements in Run 2
- Inclusive $\mu = 1.01^{+0.06}_{-0.05}$ → Good agreement with SM at current precision

Higgs boson mass m_H: H → ZZ → 4ℓ using full Run 2

Four final states: 4μ , 4e, 2μ2e, 2e2μ

Mass resolution improved by 3-8% using
beam spot constrain, Z_1 constrain, per event mass uncertainty ($\delta m_4\ell$)

Discriminant: $\delta m_{4l}/m_{4l}$ $(9\ bins)$, $\mathcal{D}_{bkg}^{kin}$

Final N −2D likelihood fit using the observables (m_{4l}, $\mathcal{D}_{bkg}^{kin}$)

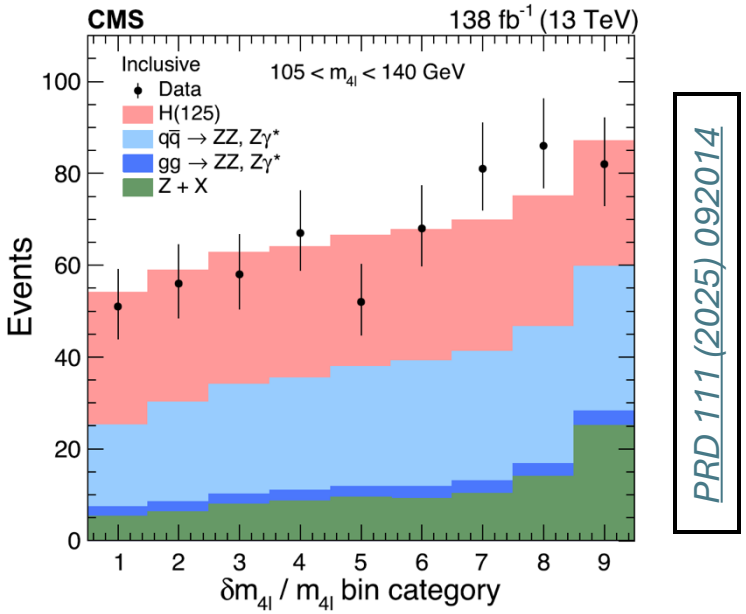

PRD 111 (2025) 092014

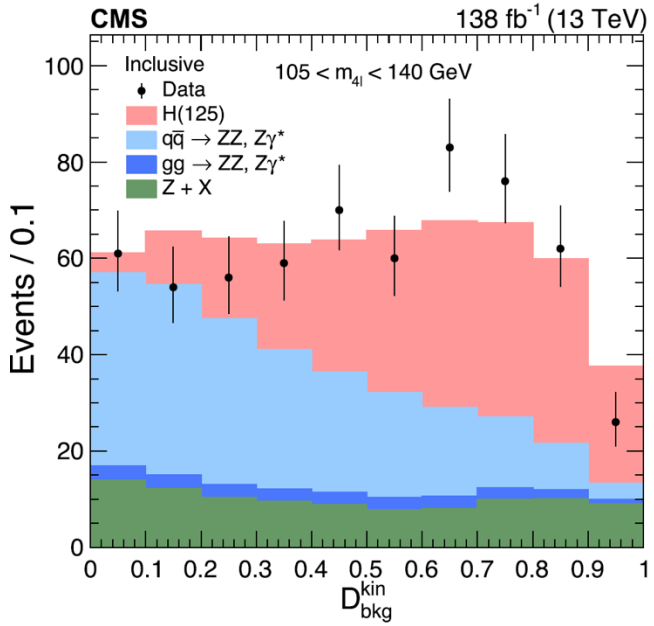

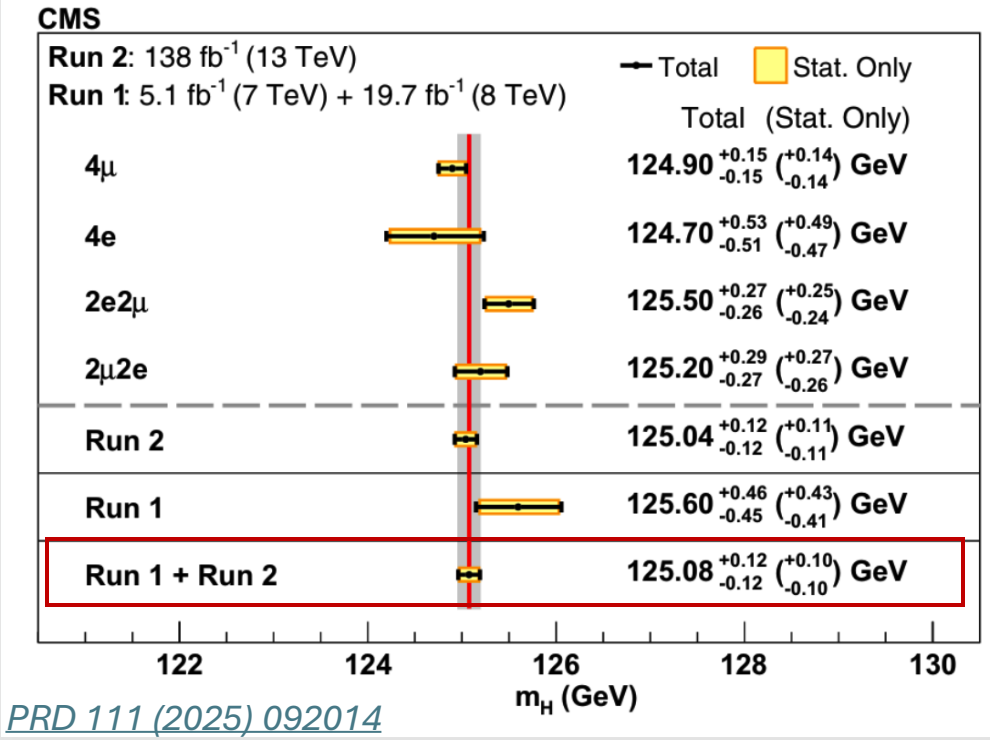

PRD 111 (2025) 092014

Most precise single channel
measurement of Higgs boson mass

$$m_H = 125.08 \pm 0.12\ \text{GeV}(\pm 0.10\ (\text{stat}) \pm 0.05\ (\text{sys})\ \text{GeV})$$

Uncertainties are mostly statistical

Higgs boson width Γ_H: H → ZZ → 4ℓ using full Run 2

Standard Model predicts narrow width
$\Gamma_H \sim 4$ MeV for $m_H \sim 125$ GeV

Invisible in the line shape since $\Gamma_{SM} \ll \sigma_m/m$ experimental resolution for $m_{\gamma\gamma}$ or $m_{4l} \sim \mathcal{O}(1)$ GeV
Direct measurement strongly limited

H → ZZ: $\Gamma_H < 50\ (330)$ MeV @ 68 (95) % CL

Indirect measurement from the ratio of on-shell and off-shell Higgs boson production

$$\frac{\sigma^{on-shell}_{gg\to H\to ZZ^*}}{\sigma^{off-shell}_{gg\to H^*\to ZZ}} \propto \frac{g_g^2 g_Z^2/m_H\Gamma_H}{g_g^2 g_Z^2/4m_Z^2} \propto \Gamma_H$$

Assumes on-shell and off-shell couplings are identical; no BSM loops in off-shell ggF

Indirect measurement in H → ZZ

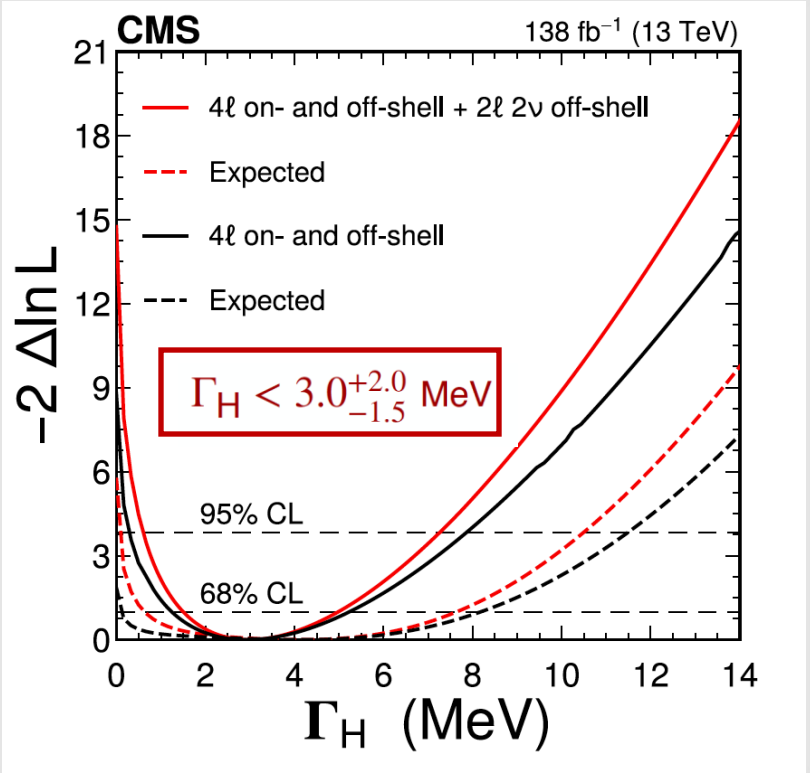

PRD 111 (2025) 092014

Production modes:
ggH, VBF, VH, ttH

Final States: 4ℓ , $2\ell 2\nu$

3 final fit observables:
$m_{4\ell}, \mathcal{D}_{bkg}, \mathcal{D}_{int}$

Simultaneous fit:
on-shell+off-shell regions

First evidence for off-shell Higgs production in ZZ.
*"no off-shell" hypothesis is excluded at **3.6σ**.*

Higgs boson width Γ_H in $H \to \gamma\gamma$ using Run 2 *(NEW results)*

A different technique, purely on-shell

New

using interference between
signal $gg \to H \to \gamma\gamma$ and QCD background $gg \to \gamma\gamma$

Signal: $\mathcal{S} \propto c_{g\gamma}^2/\Gamma_H \propto \mu$, while Interference: $\mathcal{I} \propto c_{g\gamma} = \sqrt{\mu\,\Gamma_H/\Gamma_H^{SM}}$

$gg \to H \to \gamma\gamma$ prod. | non-res. $gg \to \gamma\gamma$

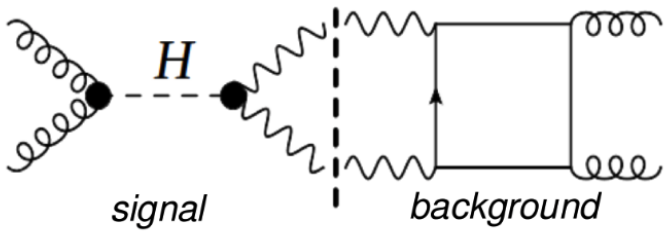

(gluon-gluon fusion)

$$|A_S + A_B|^2 = \frac{c_{g\gamma}^2}{\Gamma_H} S + c_{g\gamma} I + B$$

Interference modifies $m_{\gamma\gamma}$ spectrum
→ Its amplitude is the key to measure Γ_H

$$d\sigma_s^{ggH}/dm_{\gamma\gamma} = \frac{c_{g\gamma}^2 S}{(m_{\gamma\gamma}^2 - m_H^2)^2 + m_H^2\Gamma_H^2},$$

$$d\sigma_i/dm_{\gamma\gamma} = c_{g\gamma}\frac{(m_{\gamma\gamma}^2 - m_H^2)R + m_H\Gamma_H I}{(m_{\gamma\gamma}^2 - m_H^2)^2 + m_H^2\Gamma_H^2},$$

Signal term: Standard Breit–Wigner resonance
Interference term: Distorts invariant $m_{\gamma\gamma}$ spectrum
Real part (R): changes sign around m_H, distorts lineshape
Imag part (I): always negative, affects normalization

With detector resolution:
smeared but asymmetry
remains visible

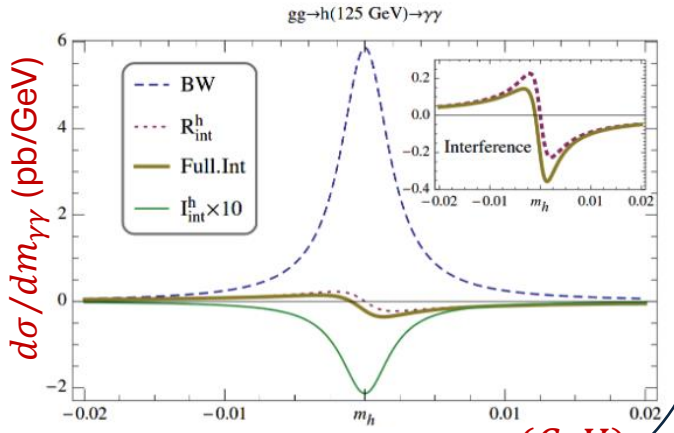

CMS PAS HIG-25-004

Higgs boson width Γ_H in $H \to \gamma\gamma$ using Run 2 *(NEW results)*

Event categorized into 11 categories
One inclusive 2j + (5 $p_{T,\gamma\gamma}$ bins x 2 diphoton BDT bins)

Phenomenology:

$$d\sigma/dm_{\gamma\gamma} = \mu_{\gamma\gamma} S + c_{g\gamma}\, I + \sum_{i \neq ggF} \mu_i\, S_i(m_{\gamma\gamma}) + B(m_{\gamma\gamma})$$

Interference contribution (sensitive to Γ_H) is negative after m_H

To handle negative interference,
the method models the full shape change of $d\sigma/dm_{\gamma\gamma}$
from S → S + I as a function of Γ_H

$$d\sigma/dm_{\gamma\gamma} = (\mu_{\gamma\gamma} - c_{g\gamma})\, S + c_{g\gamma}\,(S + I) + \sum_{i \neq ggF} \mu_i\, S_i + B(m_{\gamma\gamma})$$

Templates for $S(m_{\gamma\gamma})$ and $(S + I)\, m_{\gamma\gamma}$ from MC,
while B($m_{\gamma\gamma}$) from data sidebands

Feldman-Cousins scan
with 1000 toys for each point

New

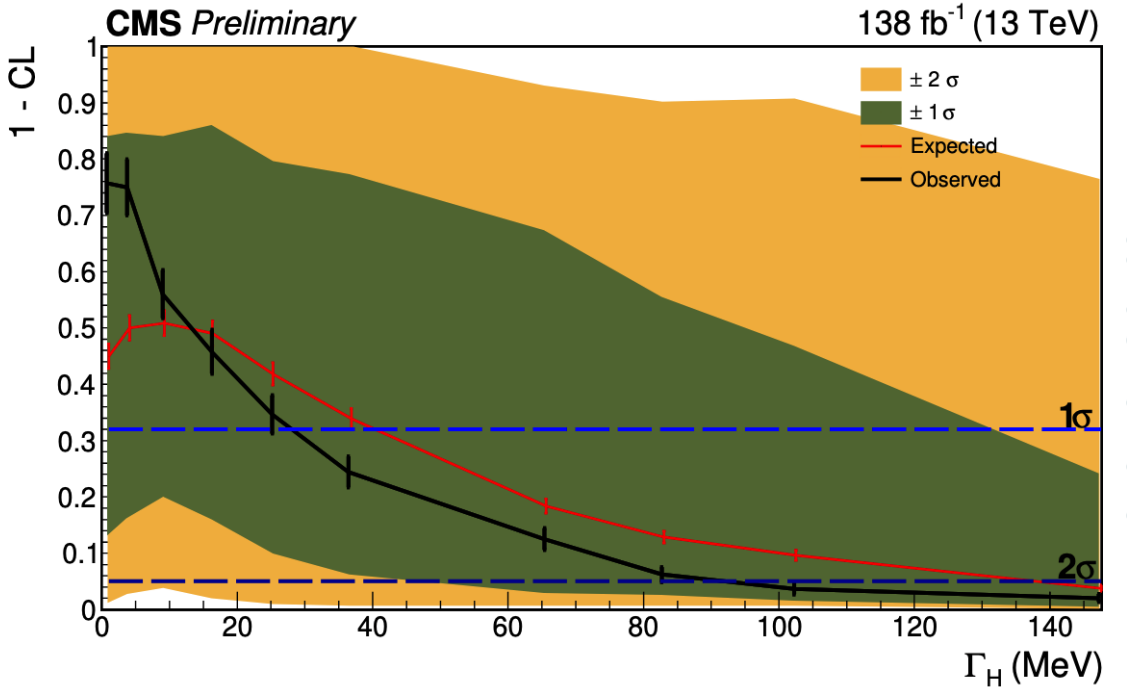

CMS PAS HIG-25-004

Limit at 95% C.L.: $\Gamma_H < 91.8$ MeV (138 MeV exp.)

Improves previous limit (Γ_H < 330 MeV from H → ZZ)

Higgs boson spin and parity: CP Structure

Higgs boson is CP even scalar in SM: $J^{CP} = 0^{++}$

Higgs boson spin-parity consistent with SM prediction

Any CP-odd interaction → BSM physics

(e.g. matter–antimatter asymmetry)

Current precision is limited

leaving room for CP-violating anomalous couplings

H : CP-even? Odd? Mixed?

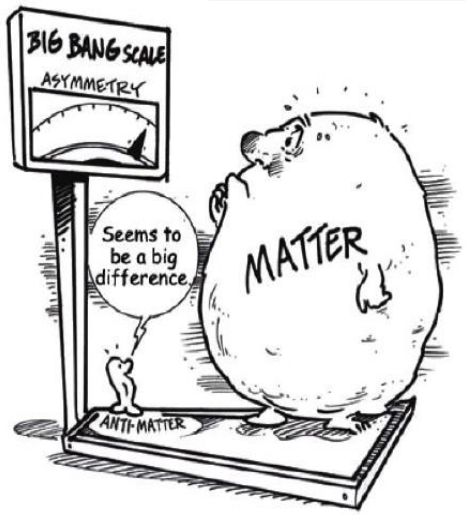

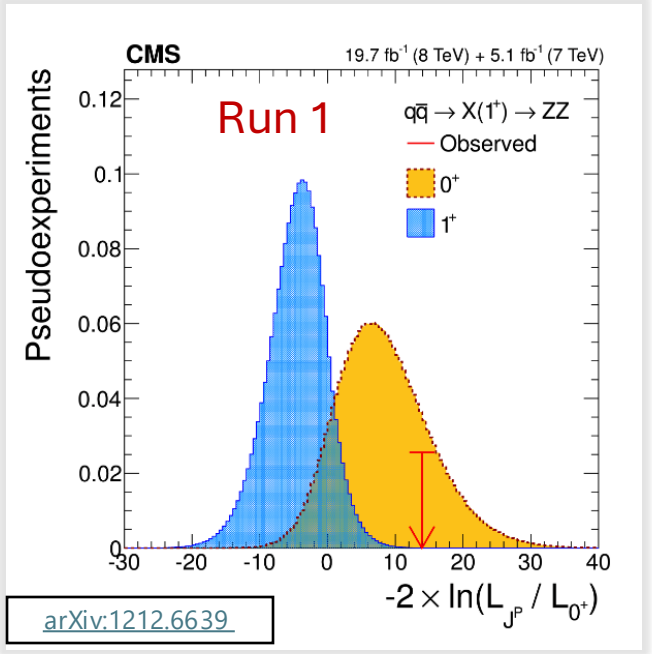

Higgs coupling to gauge boson (HVV)

$$A(HVV) \sim \left[a_1^{VV} + \frac{k_1^{VV} q_{V1}^2 + k_2^{VV} q_{V2}^2}{(\Lambda_1^{VV})^2}\right] m_{V1}^2 \epsilon_{V1}^* \epsilon_{V2}^* + a_2^{VV} f_{\mu\nu}^{*(1)} f^{*\mu\nu(2)} + a_3^{VV} f_{\mu\nu}^{*(1)} \tilde{f}^{*\mu\nu(2)}$$

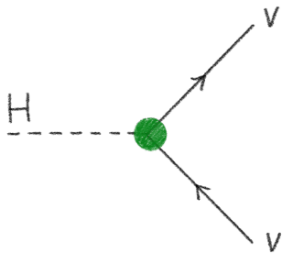

New physics scale Λ_1 ~ 1TeV

a_2 →CP even

a_3 → CP odd

AC measurements expressed in terms of **cross-section fractions**

$$f_{ai} = \frac{|a_i|^2 \sigma_i}{\sum_j |a_j|^2 \sigma_j} sign(a_i/a_1)$$

Higgs coupling to fermions (Hff)

$$A(\mathrm{Hff}) = -\frac{m_f}{v} \bar{\psi}_f \left(\kappa_f + i\tilde{\kappa}_f \gamma_5\right) \psi_f,$$

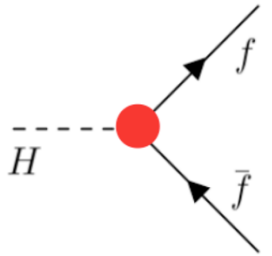

κ_f → CP even

$\tilde{\kappa_f}$ → CP odd

$$f_{CP}^{\mathrm{Hff}} = \frac{|\tilde{\kappa}_f|^2}{|\kappa_f|^2 + |\tilde{\kappa}_f|^2} \mathrm{sign}\left(\frac{\tilde{\kappa}_f}{\kappa_f}\right)$$

Anomalous Coupling in $H \rightarrow \gamma\gamma$ using full Run 2

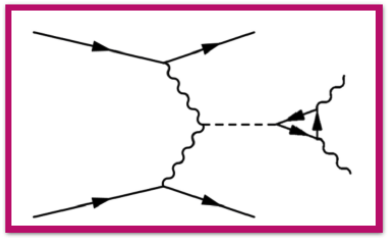

VBF ($f_{a3}, f_{a2}, f_{\Lambda_1}, f_{\Lambda_1}^{Z\gamma}$)

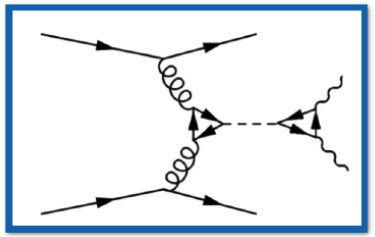

ggH+2Jets ($f_{a3}^{ggH}, f_{CP}^{Htt}$)

HVV ACs: studied in VBF & VH events

ggF ACs: from ggH + 2 jets

VBF and ggH+2j have **similar topology → separate analyses**

Categories optimized using **MELA + ML discriminants**

Goal: maximize sensitivity to CP-odd signal

2 bins each for D_{0-}^{VBF} and a pair of **DNN SM/BSM/bkg classifier** discriminants :

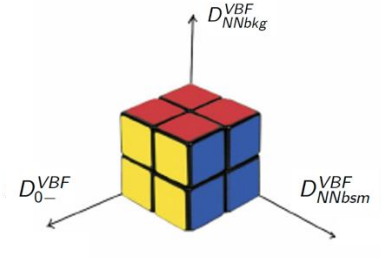

5 categories (with sufficient statistical power) included in final **HVV** analysis

ggH+2jets selection with BDT signal/bkg classifiers

3D Categorisation :

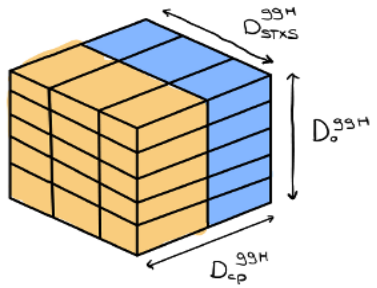

30 categories included in final H$\gamma\gamma$ analysis

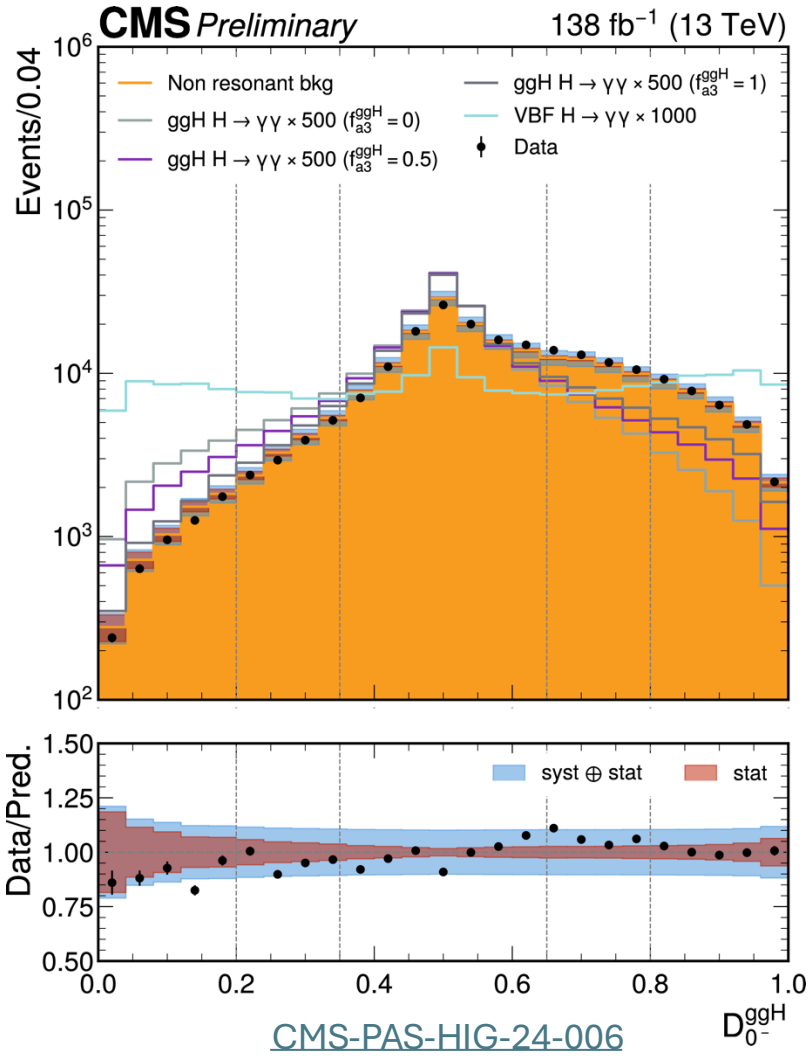

CMS-PAS-HIG-24-006

$$\mathscr{D}_{\rm BSM} = \frac{\mathscr{P}_{\rm SM}(\vec{\Omega})}{\mathscr{P}_{\rm SM}(\vec{\Omega}) + \mathscr{P}_{\rm BSM}(\vec{\Omega})} \qquad \mathscr{D}_{\rm int} = \frac{\mathscr{P}^{\rm int}_{\rm SM-BSM}(\vec{\Omega})}{\mathscr{P}_{\rm SM}(\vec{\Omega}) + \mathscr{P}_{\rm BSM}(\vec{\Omega})}$$

Anomalous Coupling in $H \rightarrow \gamma\gamma$ using full Run 2

Simultaneous maximum likelihood fit across all categories

Measures 4 HVV and 1 Hgg anomalous coupling (AC) cross-section ratios

No significant deviations from SM predictions are observed

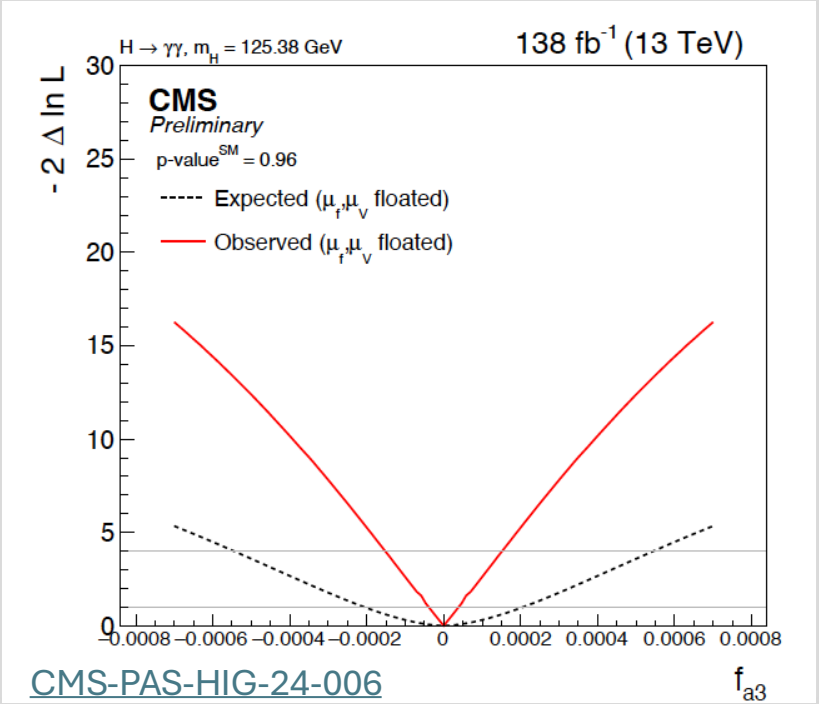

CMS-PAS-HIG-24-006

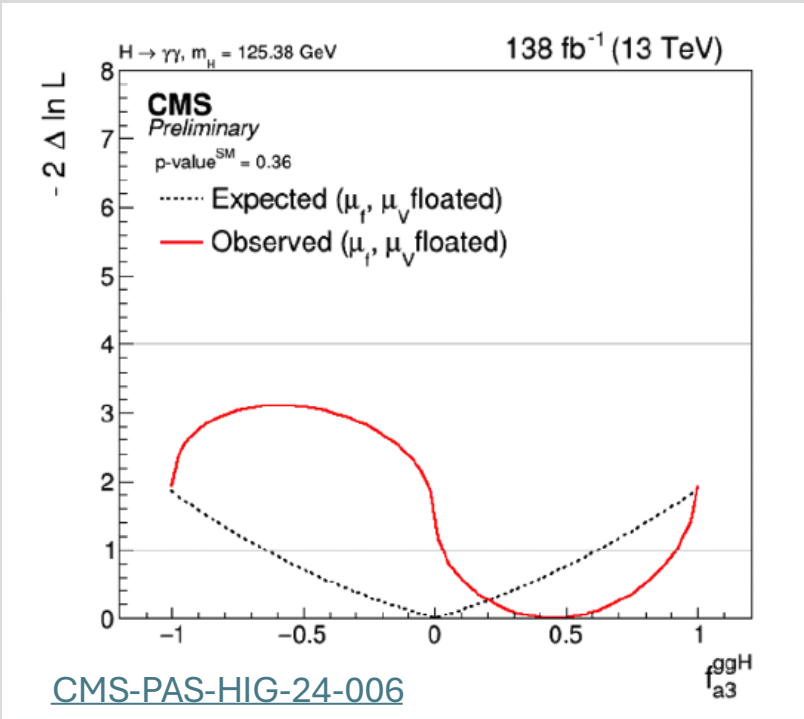

CMS-PAS-HIG-24-006

*Parameter	Expected/(10^{-4}) $H \rightarrow \gamma\gamma$ (68% CL)	Observed/(10^{-4}) $H \rightarrow \gamma\gamma$ (68% CL)
f_{a3}	$0.0^{2.1}$	$0.00^{0.39}$
f_{a2}	$0.0^{+3.1}_{-2.3}$	$-0.81^{+0.65}_{-2.0}$
$f_{\Lambda 1}$	$0.0^{+0.35}_{-0.12}$	$-0.014^{+0.032}_{-0.14}$
$f_{\Lambda 1}$	$0.0^{+3.7}_{-3.3}$	$0.83^{+1.5}_{-0.92}$

Parameter	Expected/(68% CL)	Observed/(68% CL)
f_{a3}^{ggH}	$0.00^{+0.63}_{-0.65}$	$0.45^{+0.47}_{-0.43}$
f_{CP}^{ggH}	$0.00^{+0.50}_{-0.50}$	$0.26^{+0.56}_{-0.26}$

First CMS cross-sections using Run 3 (2022)

First CMS cross section measurement at 13.6 TeV using 2022 data with 34.7 fb^{-1}

fiducial phase space was defined to reduce model dependence

differential cross section as function of p_T^H *and* $|y_H|$

measured inclusive fiducial cross section in different final states ($\gamma\gamma$ or ZZ: 4μ, 2e2μ, 4e)

$H \rightarrow \gamma\gamma$

arXiv:2504.17755

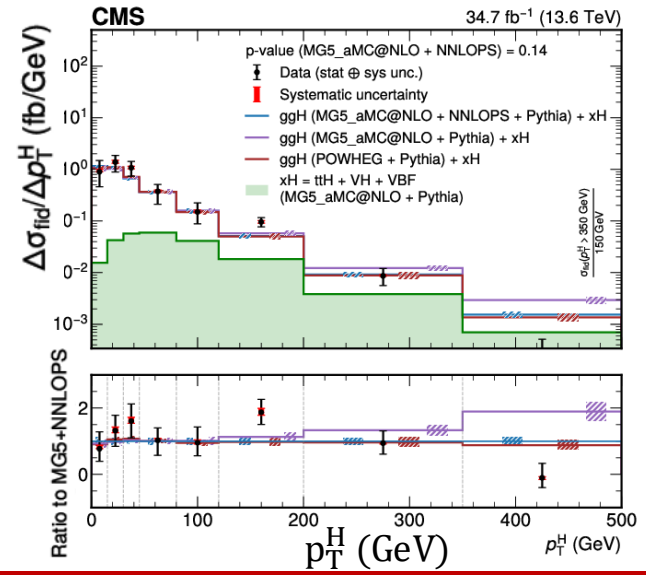

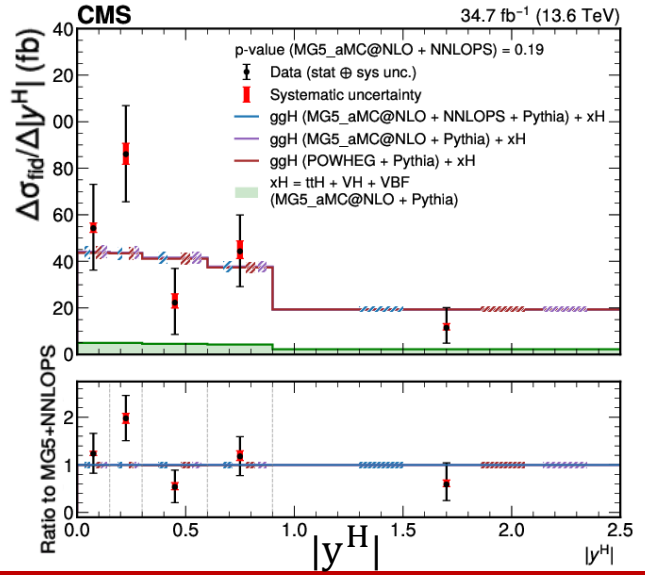

$H \rightarrow ZZ \rightarrow 4l$

J. High Energ. Phys. **2025**, 79

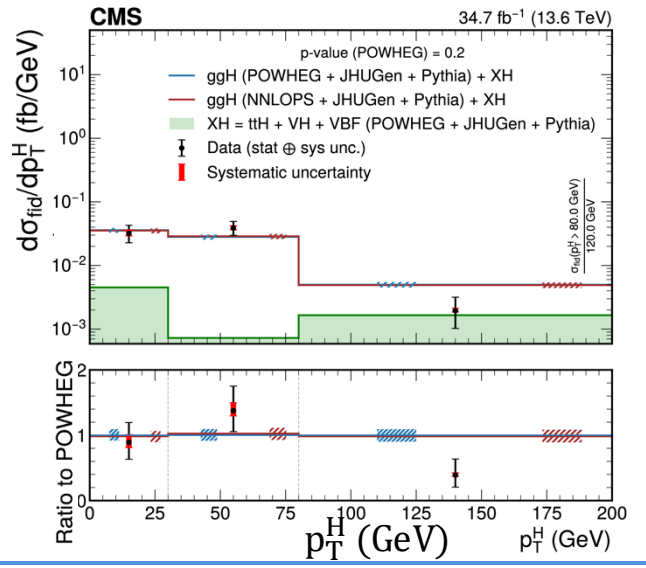

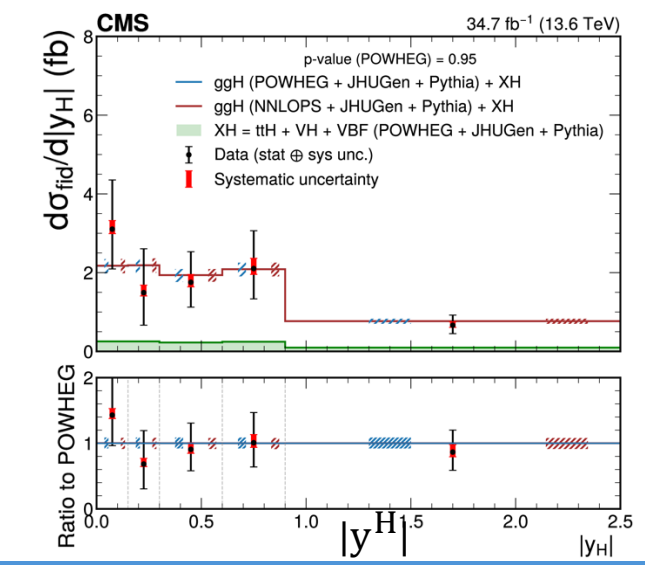

First CMS cross-sections using Run 3 (2022)

Inclusive cross-section in $H \rightarrow \gamma\gamma$ & $H \rightarrow ZZ \rightarrow 4l$

$H \rightarrow \gamma\gamma$

$$\sigma_{\text{fid}}^{\gamma\gamma} = 74 \pm 11\ (\text{stat})\ ^{+5}_{-4}\ (\text{syst})\ \text{fb}$$

$$\sigma_{\text{fid}}^{\gamma\gamma}\ (\text{exp}) = 67.8 \pm 3.8\ \text{fb}$$

$H \rightarrow ZZ \rightarrow 4l$

$$\sigma_{\text{fid}}^{ZZ} = 2.89\ ^{+0.53}_{-0.49}\ (\text{stat})\ ^{+0.29}_{-0.21}\ (\text{syst})\ \text{fb}$$

$$\sigma_{\text{fid}}^{ZZ}\ (\text{exp}) = 3.09\ ^{+0.27}_{-0.24}\ \text{fb}$$

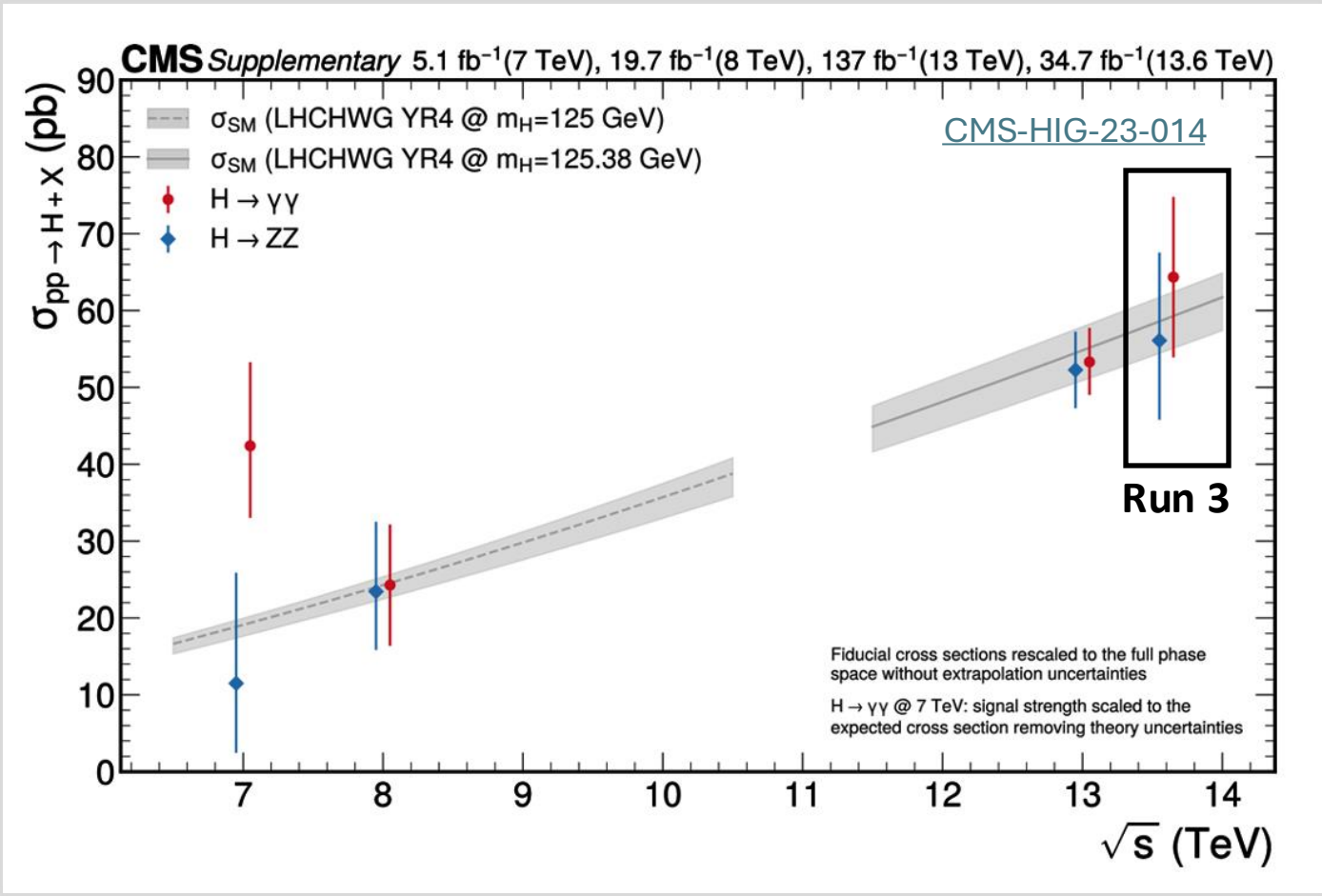

Summary & Outlook

Recent CMS analyses have provided significant new measurements that enhance our understanding of the Higgs boson's properties.

Mass: Measured with ~0.1% precision (0.12 GeV); most precise from $H \rightarrow ZZ \rightarrow 4\ell$

Width: Direct measurement limited; best constraints from indirect measurements of on-shell/off-shell in H → ZZ; New upper limit is set by $H \rightarrow \gamma\gamma$ using interferences effects, representing the first purely on-shell width measurement.

CP & ACs: Searches for anomalous or CP-violating couplings in $H \rightarrow \gamma\gamma$ *decay mode for first time* show no significant deviations; results consistent with CP-even SM Higgs

Cross-sections: First look at Run3 for the cross-sections measurement of Higgs using 2022 data with 34.7 fb^{-1} in H → ZZ & $H \rightarrow \gamma\gamma$ *channel*

Higgs remains SM-like, but HL-LHC offers more opportunities for precision and new discovery.

Stay tuned!

Thank you very much for your attention!

CMS Higgs Property Measurements Discussed

Property	CMS ID	Final State	√s (TeV)	Luminosity	Run
Mass	HIG-21-019	$H \to ZZ \to 4\ell$	13.0	138 fb^{-1}	Run 2
Width	HIG-21-019	$H \to ZZ \to 4\ell$ (on-/off-shell)	13.0	138 fb^{-1}	Run 2
	HIG-25-004	$H \to \gamma\gamma$ (NEW on-shell)			
SP / CP / Anomalous coupling	HIG-24-006	$H \to \gamma\gamma$	13.0	138 fb^{-1}	Run 2
Cross-section	HIG-23-014	$H \to \gamma\gamma$	13.6	~35 fb^{-1}	Run 3
	HIG-24-013	$H \to ZZ \to 4\ell$			

Compact Muon Solenoid (CMS) Experiment at LHC

CMS Detectors:

- Silicon Tracker
- Electromagnetic Calorimeter
- Hadron Calorimeter
- Muon System

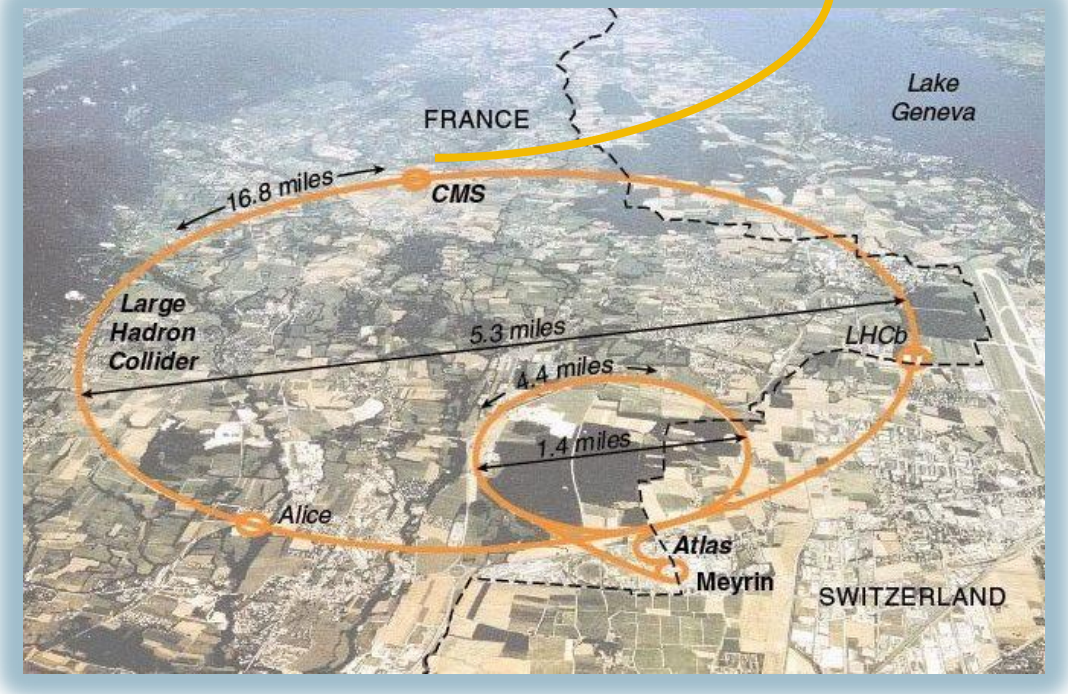

CMS DETECTOR

Total weight	: 14,000 tonnes
Overall diameter	: 15.0 m
Overall length	: 28.7 m
Magnetic field	: 3.8 T

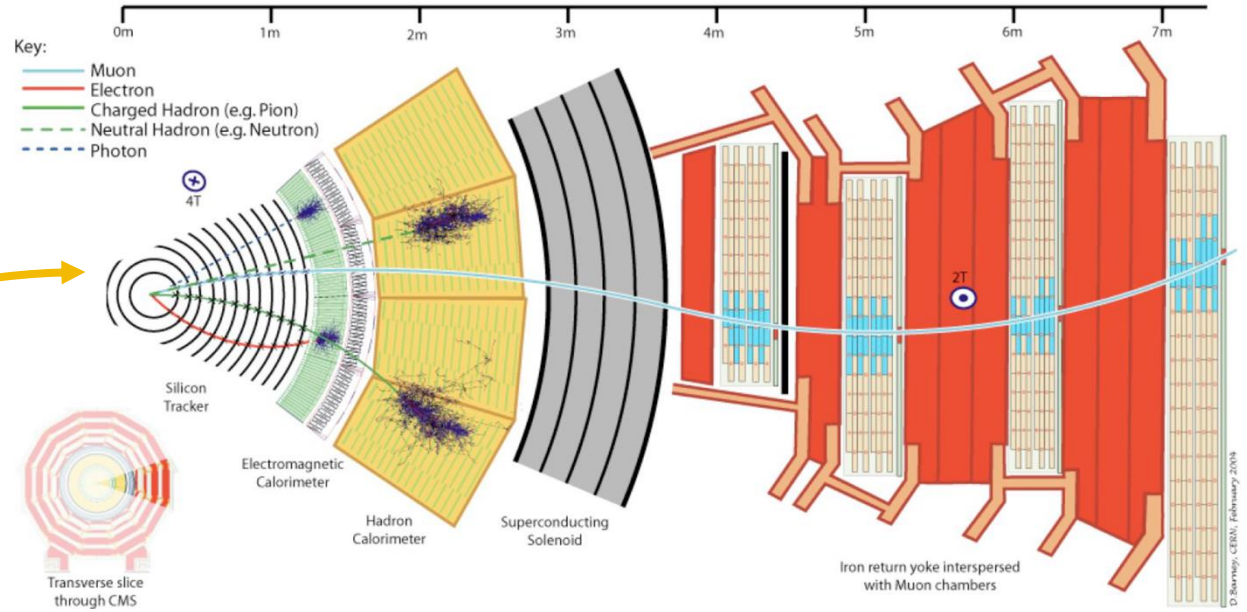

Common analysis strategies:

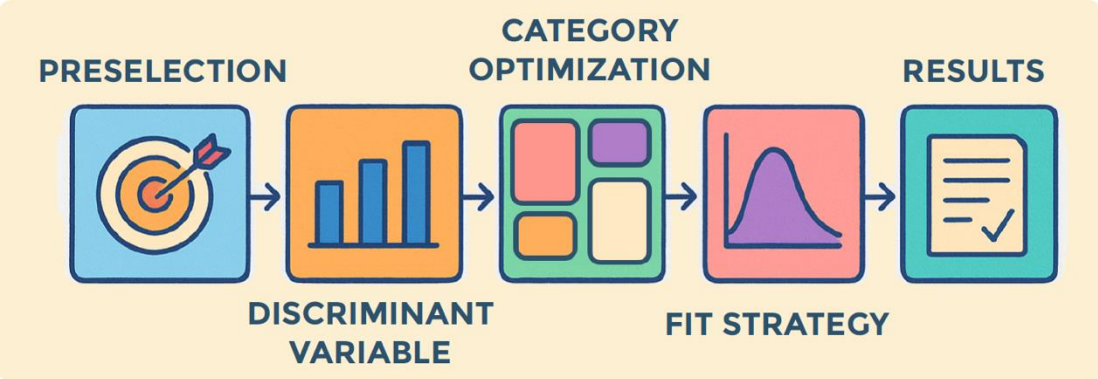

Higgs Boson Production and Decay modes

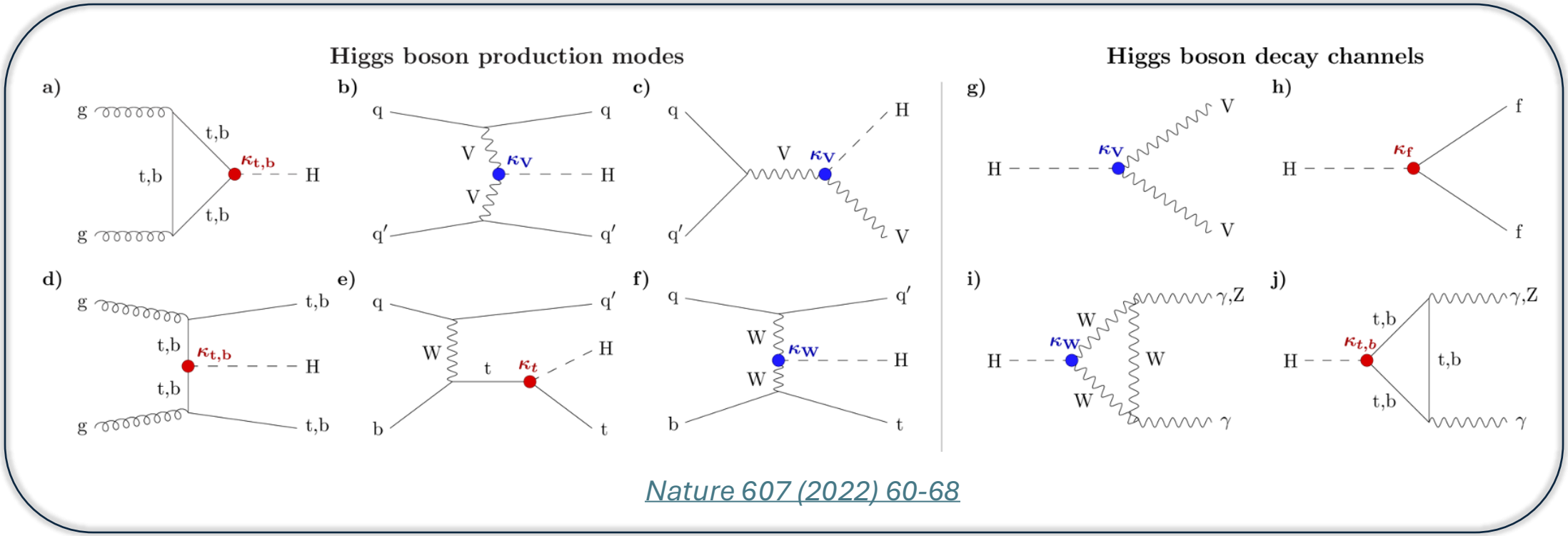

Nature 607 (2022) 60-68

$$\mu = \frac{\sigma \cdot \mathcal{B}}{\sigma_{SM} \cdot \mathcal{B}_{SM}} = \frac{Observed\ event\ rate}{SM\ Expected\ rate} \begin{cases} \mu = 1: observed\ data\ is\ consistent\ with\ SM\ predictions \\ \mu \neq 1: observed\ data\ deviates\ from\ SM; suggesting\ potential\ new\ physics \end{cases}$$

Improving $m_4\ell$ Resolution in H → ZZ → 4ℓ CMS-HIG-21-019

- **Beam Spot (BS) Constraint**
  - Common BS point in track reconstruction
  - **Muons**: p_t recalculated → resolution gain
  - **Electrons**: unaffected (ECAL-dominated)
  - → Improves $m_4\ell$ resolution by **3–8%**
- **Event-by-Event Mass Uncertainty ($\delta m_4\ell$)**
  - Derived from per-lepton momentum uncertainties
  - Muons → covariance matrix of track fit
  - Electrons → ECAL + tracker (neglect track direction)
  - $\delta m_4\ell = \sqrt{\Sigma(\delta m_{i4}\ell)^2}$
- **Calibration of $\delta m_4\ell$**
  - Corrections derived in $|\eta|$ and ($\delta p_t/p_t$, $|\eta|$) bins
  - 2ℓ mass fits:
    - Breit–Wigner (Z) ⊗ Double-Sided Crystal Ball (detector) + exponential (background)
  - Closure test ensures consistency
- **Kinematic Fit with Z_1 Mass Constraint**

  → Further improvement in Higgs mass resolution
  - Refits leptons from Z_1 → follow true Z line shape
  - Adjusts lepton momenta via likelihood

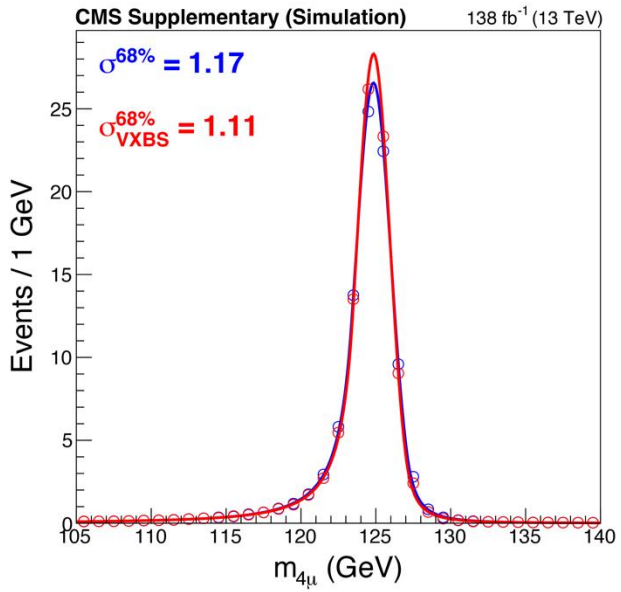

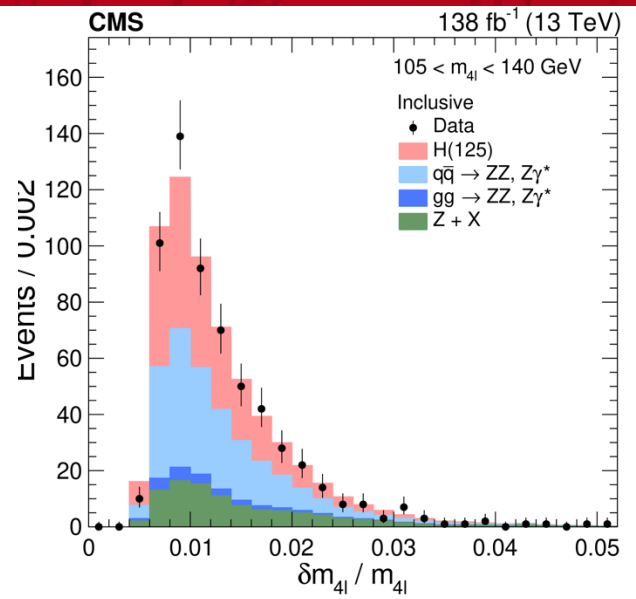

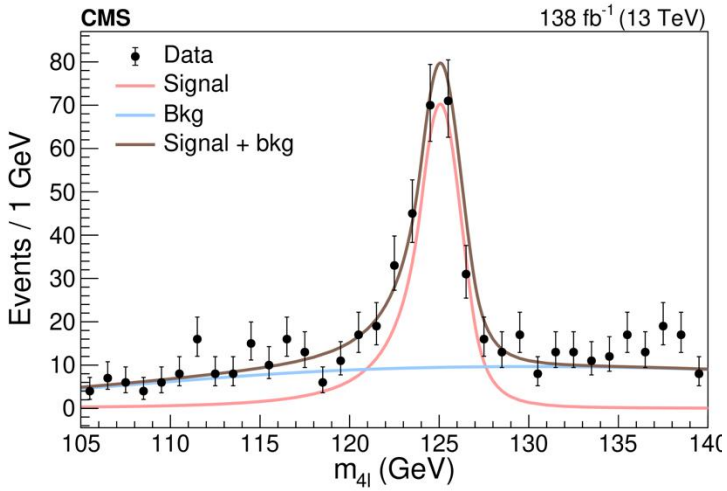

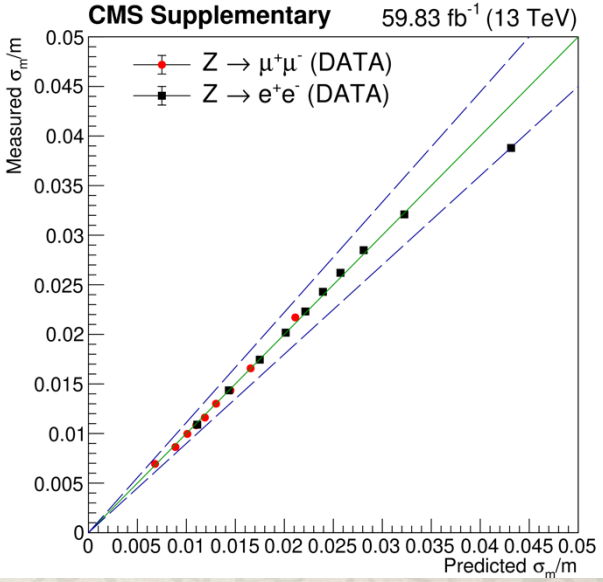

CMS-HIG-21-019

Kinematic Discriminants (MELA)

Motivation: Use matrix elements to compute event-by-event probabilities for different physics hypotheses

- Higgs → 4ℓ + jets described by up to 13 observables (Ω)
- Higgs → 4ℓ + jets described by up to 7 observables (Ω)
- **MELA** (Matrix Element Likelihood Approach) framework

reduces dimensionality → optimal sensitivity

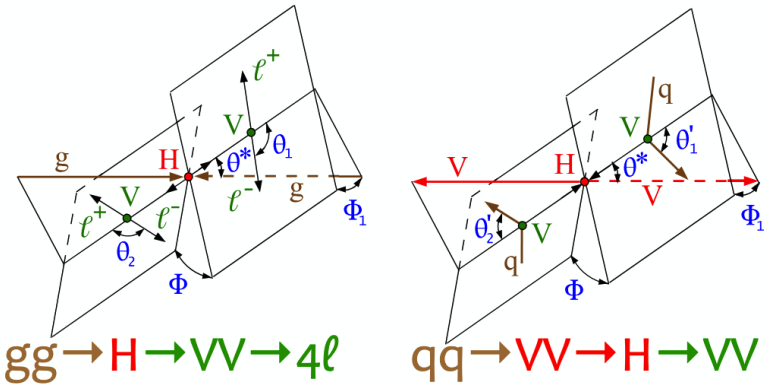

MELA Discriminants:

- **Alternative model vs. signal:** Separates SM-like Higgs events from alternative or background scenarios

$$\mathscr{D}_{\rm alt}(\boldsymbol{\Omega}) = \frac{\mathscr{P}_{\rm sig}(\boldsymbol{\Omega})}{\mathscr{P}_{\rm sig}(\boldsymbol{\Omega}) + \mathscr{P}_{\rm alt}(\boldsymbol{\Omega})}$$

- **Interference term:** it separate whether an observed event is consistent with **constructive**, **destructive**, or **no interference** between the signal and alternative amplitudes. **(Sign sensitive)**

$$\mathscr{D}_{\rm int}(\boldsymbol{\Omega}) = \frac{\mathscr{P}_{\rm int}(\boldsymbol{\Omega})}{2\sqrt{\mathscr{P}_{\rm sig}(\boldsymbol{\Omega})\mathscr{P}_{\rm alt}(\boldsymbol{\Omega})}},$$

$$\mathcal{P}_H(\Omega) \propto |\mathcal{M}_H(\Omega)|^2$$

$$\mathcal{P}_{\rm int}(\Omega) \propto 2\,\mathrm{Re}\left[\mathcal{M}_{\rm sig}\,\mathcal{M}^*_{\rm alt}\right]$$

➢ Method:

- Starts from the reconstructed event
- Extracts observables (Ω)
- Computes matrix-element probabilities ($|\mathcal{M}_H(\Omega)|^2$)
- Produces per-event likelihoods ($\mathcal{P}_{sig}, \mathcal{P}_{alt}$)
- Builds discriminants ($\mathcal{D}_{alt}, \mathcal{D}_{int}$)
- Feeds into event categorization and fits

H → ZZ → 4ℓ CMS-HIG-21-019

On-shell measurements: $\mathscr{P}_{jk}(\vec{x};\vec{\xi}_{jk},\vec{\zeta}) = \mu_j \mathscr{P}^{\mathrm{sig}}_{jk}(\vec{x};\vec{\xi}_{jk},\vec{\zeta}) + \mathscr{P}^{\mathrm{bkg}}_{jk}(\vec{x};\vec{\xi}_{jk}),$

$$\mathscr{P}_{\mathrm{2D}}(m_{4\ell}, \mathscr{D}^{\mathrm{kin}}_{\mathrm{bkg}}) = \mathscr{P}^{\mathrm{sig}}_{\mathrm{1D}} T^{\mathrm{sig}}(\mathscr{D}^{\mathrm{kin}}_{\mathrm{bkg}} | m_{4\ell}) + \mathscr{P}^{\mathrm{bkg}}_{\mathrm{1D}} T^{\mathrm{bkg}}(\mathscr{D}^{\mathrm{kin}}_{\mathrm{bkg}} | m_{4\ell}).$$

PRD 111 (2025) 092014

Off-shell measurements: m_{4l} > 220 GeV PRD 111 (2025) 092014

Category	VBF-tagged	VH-tagged	Untagged
Selection	$\mathscr{D}^{\mathrm{VBF}}_{\mathrm{2jet}} > 0.5$	$\mathscr{D}^{ZH}_{\mathrm{2jet}}$ or $\mathscr{D}^{WH}_{\mathrm{2jet}} > 0.5$	Rest of the events
Observables	$m_{4\ell}$, $\mathscr{D}^{\mathrm{VBF+dec}}_{\mathrm{bkg}}$, $\mathscr{D}^{\mathrm{VBF+dec}}_{\mathrm{bsi}}$	$m_{4\ell}$, $\mathscr{D}^{VH+\mathrm{dec}}_{\mathrm{bkg}}$, $\mathscr{D}^{VH+\mathrm{dec}}_{\mathrm{bsi}}$	$m_{4\ell}$, $\mathscr{D}^{\mathrm{kin}}_{\mathrm{bkg}}$, $\mathscr{D}^{\mathrm{gg,dec}}_{\mathrm{bsi}}$

$$\mathscr{P}_{jk}(\vec{x};\vec{\xi}_{jk},\vec{\zeta}) = \frac{\mu_j \Gamma_H}{\Gamma_0}\mathscr{P}^{\mathrm{sig}}_{jk}(\vec{x};\vec{\xi}_{jk}) + \sqrt{\frac{\mu_j \Gamma_H}{\Gamma_0}}\mathscr{P}^{\mathrm{int}}_{jk}(\vec{x};\vec{\xi}_{jk}) + \mu_j \mathscr{P}^{\mathrm{cross}}_{jk}(\vec{x};\vec{\xi}_{jk}) + \mathscr{P}^{\mathrm{bkg}}_{jk}(\vec{x};\vec{\xi}_{jk}),$$ PRD 111 (2025) 092014

On-shell ZH events with H→WW/ZZ producing extra leptons
ZH Cross-Feed events removed from Off-Shell Region **to avoid double counting**

PRD 111 (2025) 092014

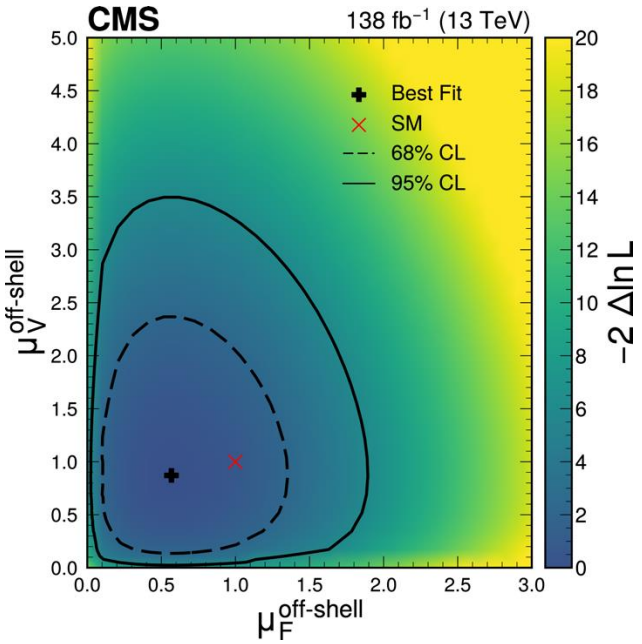

Largest Systematics:
On-shell: from **lepton momentum scale & resolution**;
Off-shell: dominated by QCD background modeling and **jet energy calibration** in VBF/VH categories.

Higgs boson width Γ_H in $H \rightarrow \gamma\gamma$ using Run 2 *(NEW results)*

- In the narrow-width approximation (NWA), $\sigma_{i\rightarrow H\rightarrow f} \sim \frac{g_i^2\, g_f^2}{\Gamma_H}$
- Scaling degeneracy: If $g = \lambda g^{SM}$ & $\Gamma_H = \lambda^4 \Gamma_H^{SM}$ then $\sigma_{i\rightarrow H\rightarrow f} = \sigma_{i\rightarrow H\rightarrow f}^{SM}$
- Consequence for LHC data:

  On-shell Higgs cross sections **cannot determine** absolute Higgs couplings or the total width

  Many different λ values give the same measured rates.

  Only **ratios** of couplings are constrained by on-shell measurements
- Breaking the degeneracy (extra information needed):

  Use **off-shell Higgs production** (gg→H→ZZ at high mass).

  Study **interference effects** between Higgs and background.

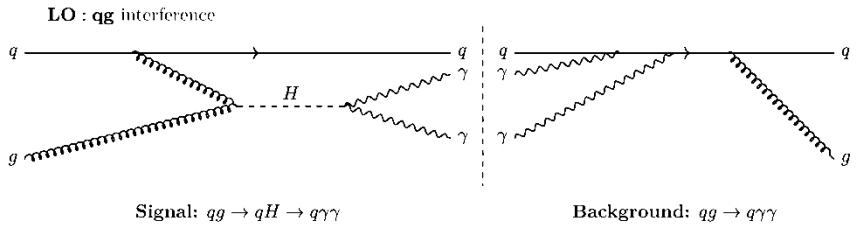

Method 1:
Mass peak shift

Method 2:
Full shape change

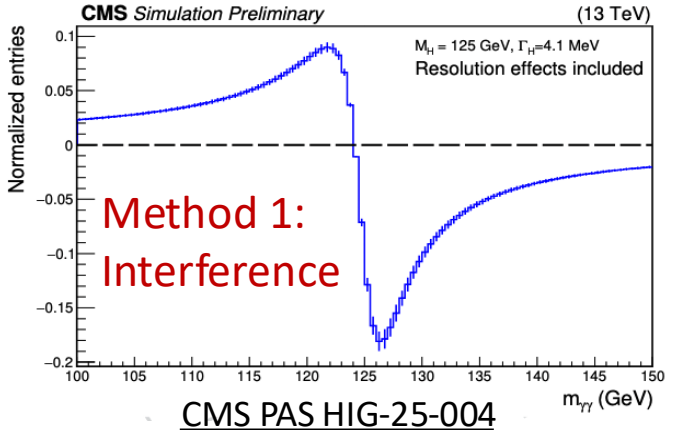

CMS PAS HIG-25-004

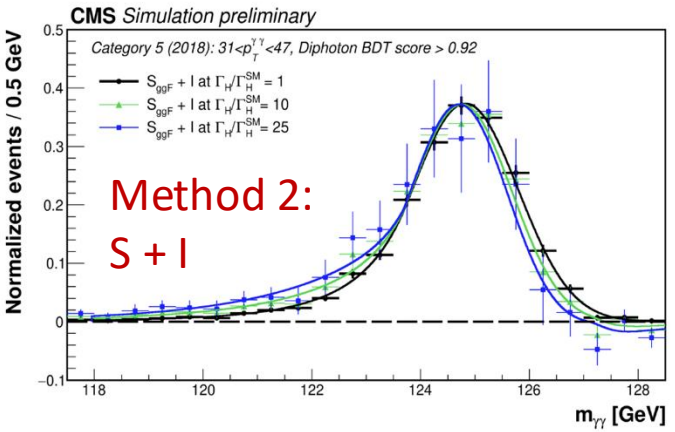

Higgs boson width Γ_H in $H \to \gamma\gamma$ using Run 2 *(NEW results)*

$$\mathcal{A}_{gg\to\gamma\gamma} = \frac{-\mathcal{A}_{gg\to H}\mathcal{A}_{H\to\gamma\gamma}}{\hat{s} - m_H^2 + i m_H \Gamma_H} + \mathcal{A}_{\text{cont}}$$

$$\delta\hat{\sigma}_{gg\to H\to\gamma\gamma} = -2(\hat{s} - m_H^2)\frac{\text{Re}\left(\mathcal{A}_{gg\to H}\mathcal{A}_{H\to\gamma\gamma}\mathcal{A}^*_{\text{cont}}\right)}{(\hat{s} - m_H^2)^2 + m_H^2\Gamma_H^2} - 2m_H\Gamma_H\frac{\text{Im}\left(\mathcal{A}_{gg\to H}\mathcal{A}_{H\to\gamma\gamma}\mathcal{A}^*_{\text{cont}}\right)}{(\hat{s} - m_H^2)^2 + m_H^2\Gamma_H^2}$$

$$\frac{d\sigma_s^{ggH}}{dm_{\gamma\gamma}} + \frac{d\sigma_i}{dm_{\gamma\gamma}} + \frac{d\sigma_s^{V}}{dm_{\gamma\gamma}} + \frac{d\sigma_b}{dm_{\gamma\gamma}} =$$

$$\left(\mu_F - \sqrt{\mu_F\frac{\Gamma_H}{\Gamma_H^{SM}}}\right)\mathcal{S}_{ggH} + \sqrt{\mu_F\frac{\Gamma_H}{\Gamma_H^{SM}}}(\mathcal{S}_{ggH} + \mathcal{I}) + \mu_V\sum_{j\in\{\text{VBF, VH}\}}\mathcal{S}_{V,j} + \frac{d\sigma_b}{dm_{\gamma\gamma}}$$

$$N_k(i, \Gamma_H/\Gamma_H^{SM}, \vec{\mu}, m_H, \vec{\theta}) = \sum_j^{procs}\mu_j(\Gamma_H/\Gamma_H^{SM})n_{j,k}P_{jk}^{\text{sig}}\left(x_i, m_H; \vec{\theta}\right) + P_k^{\text{bkg}}\left(x_i; \vec{\theta}\right)$$

$$\mathcal{L}\left(\text{data} \mid \Gamma_H/\Gamma_H^{SM}, \vec{\mu}, m_H, \vec{\theta}_S, \vec{\theta}_B\right) = \prod_{k=1}^{n_{\text{cat}}}\prod_{i=1}^{n_{bins}}\text{Pois}\left(n_{ki}^{\text{data}} \mid N_k(i, \Gamma_H/\Gamma_H^{SM}, \vec{\mu}, m_H, \vec{\theta})\right)$$

The largest experimental systematics: non-linearity in the photon energy scale

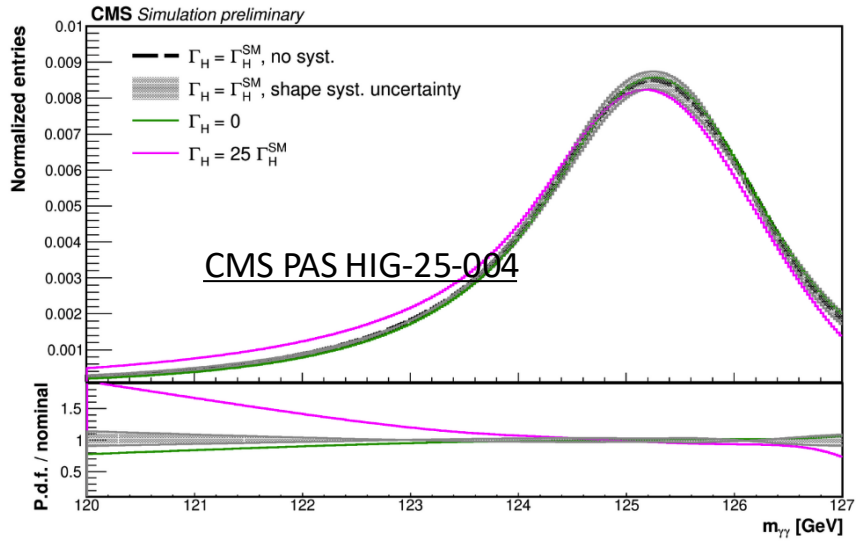

Fit uses floating signal strengths: μF (ggH), μV (VBF/VH)
Define parameter: $\lambda = \sqrt{\Gamma_H/\Gamma_H^{SM}}$
Benefits:
- Avoids discontinuity at Γ_H =0
- λ can be negative → models fluctuations better

Limits on λ → converted to limits on Γ_H

Anomalous Coupling in $H \to \gamma\gamma$ using full Run 2

Production mode	Discr.	Goal
ggH	$\mathcal{D}_{0-}^{ggH}$	CP-even VS CP-odd scenarios
ggH	$\mathcal{D}_{CP}^{ggH}$	Probe the interference
ggH	$\mathcal{D}_{STXS}^{ggH}$	Higgs signal VS non-resonant background
ggH	$\mathcal{D}_{bkg}^{ggH+2jets}$	ggH + 2 jets (SM and CP-odd) VS rest
ggH	$\mathcal{D}_{BSM}^{ggH+2jets}$	ggH + 2 jets (CP-odd) VS rest
VBF	$\mathcal{D}_{0-}^{VBF}$	SM VS CP-odd scenarios
VBF	$\mathcal{D}_{NNbkg}^{VBF}$	Higgs signal VS non-resonant background
VBF	$\mathcal{D}_{NNBSM}^{VBF}$	SM Higgs VS BSM Higgs
VH-hadronic	$\mathcal{D}_{bkg}^{had}$	Higgs signal VS non-resonant background
VH-hadronic	$\mathcal{D}_{BSM}^{had}$	SM Higgs VS BSM Higgs
W($\ell\nu$)-leptonic	$\mathcal{D}_{STXS}^{lep}$	Higgs signal VS non-resonant background
W($\ell\nu$)-leptonic	$\mathcal{D}_{BSM}^{lep}$	SM Higgs VS BSM Higgs
Z($\ell\ell$)-leptonic	$\mathcal{D}_{STXS}^{lep}$	Higgs signal VS non-resonant background
Z($\ell\ell$)-leptonic	$\mathcal{D}_{BSM}^{lep}$	SM Higgs VS BSM Higgs
Z($\nu\nu$)-MET	$\mathcal{D}_{STXS}^{MET}$	Higgs signal VS non-resonant background
Z($\nu\nu$)-MET	$\mathcal{D}_{BSM}^{MET}$	SM Higgs VS BSM Higgs

CMS-PAS-HIG-24-006

$$P_{jk}^{sig}(m_{\gamma\gamma};\vec{\theta_{jk}},f_i) = (1-f_i)P_{jk}^{a_1}(m_{\gamma\gamma};\vec{\theta_{jk}}) + f_i P_{jk}^{i}(m_{\gamma\gamma};\vec{\theta_{jk}}) + 2\sqrt{f_i(1-f_i)}cos(\phi_{ai})P_{jk}^{a_1,a_i}(m_{\gamma\gamma};\vec{\theta_{jk}})$$

$$\Omega^{prod} = \{\theta_1^{prod}, \theta_2^{prod}, \theta^{*prod}, \Phi^{prod}, \Phi_1^{prod}, p_1^{2,Vprod}, p_2^{2,prod}\}$$

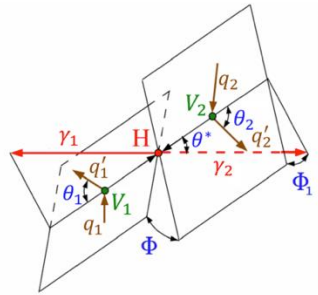

$$\mathcal{D}_{BSM} = \frac{\mathcal{P}_{SM}(\vec{\Omega})}{\mathcal{P}_{SM}(\vec{\Omega}) + \mathcal{P}_{BSM}(\vec{\Omega})}$$

$$\mathcal{D}_{int} = \frac{\mathcal{P}_{SM-BSM}^{int}(\vec{\Omega})}{\mathcal{P}_{SM}(\vec{\Omega}) + \mathcal{P}_{BSM}(\vec{\Omega})}$$

$$|f_{CP}^{Hff}| = \left(1 + 2.38\left[\frac{1}{|f_{a3}^{ggH}|} - 1\right]\right)^{-1}$$

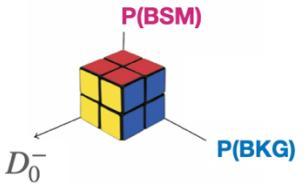

Systematic Uncertainties in H→γγ

- Experimental (line shape):
  - jet energy scale/smearing → ~15%
- Experimental (normalization):
  - Photon energy scale & resolution → ~5%
- Theoretical:
  - PDF uncertainty → ~20%

Overall: systematics <10% of total uncertainty (statistics dominate)

$$\sigma = \sum_{i=1}^{8}\left(\frac{S_{VBF}^{BSM}}{\sqrt{B}}\right) \qquad SF = \frac{N_{data}^{CR}}{N_{MC}^{CR}}$$

$$\sigma = \sum_{i=1}^{8}\left(\frac{f_{a3}\cdot N_{a3}^{VBF}}{\sqrt{SF\times N_{BKG}^{non-res} + (1-f_{a3})\times N_{SM}^{VBF} + N_{BKG}^{res}}}\right)$$

$$N_{VBF} = \mu[(1-f_{a_3})\times N_{VBF}^{SM} + f_{a_3}N_{VBF}^{a3}]$$

Use as f_{a_3} upper limit from: HIG-19-009

OPTIMAL BOUNDARIES:
P(BSM) = 0.97
P(BKG) = 0.05
D_0^- = 0.6

Categories VBF BSM dominated | Categories VBF SM dominated

8 = 2 + 2 + 1 + 3

Categories BKG Dominated | Empty